

# Editable-DeepSC: Reliable Cross-Modal Semantic Communications for Facial Editing

Bin Chen, Wenbo Yu, Qinshan Zhang, and Shu-Tao Xia

**Abstract**—Real-time computer vision (CV) plays a crucial role in various real-world applications, whose performance is highly dependent on communication networks. Nonetheless, the data-oriented characteristics of conventional communications often do not align with the special needs of real-time CV tasks. To alleviate this issue, the recently emerged semantic communications only transmit task-related semantic information and exhibit a promising landscape to address this problem. However, the communication challenges associated with Semantic Facial Editing, one of the most important real-time CV applications on social media, still remain largely unexplored. In this paper, we fill this gap by proposing Editable-DeepSC, a novel cross-modal semantic communication approach for facial editing. Firstly, we theoretically discuss different transmission schemes that separately handle communications and editings, and emphasize the necessity of Joint Editing-Channel Coding (JECC) via iterative attributes matching, which integrates editings into the communication chain to preserve more semantic mutual information. To compactly represent the high-dimensional data, we leverage inversion methods via pre-trained StyleGAN priors for semantic coding. To tackle the dynamic channel noise conditions, we propose SNR-aware channel coding via model fine-tuning. Extensive experiments indicate that Editable-DeepSC can achieve superior editings while significantly saving the transmission bandwidth, even under high-resolution and out-of-distribution (OOD) settings.

**Index Terms**—Semantic communications, cross-modal data, facial editing tasks, generative adversarial networks.

## I. INTRODUCTION

IN the era of rapid technological advancement, real-time computer vision (CV) plays a pivotal role in various real-world applications, such as digital manufacturing [2], telemedicine [3], robotics [4], and metaverse [5]. The performance of real-time CV tasks is heavily dependent on the underlying communication networks. These traditional communication systems are primarily designed for data-oriented purpose and focus on metrics that measure the data transmission instead of the tasks execution performance. In other words, the original data is expected to be completely recovered at the receiver side regardless of the users’ usage about it. Nonetheless, this data-oriented design principle is not always suitable for the specific needs of real-time CV tasks, as different tasks at the receiver side would require different types of

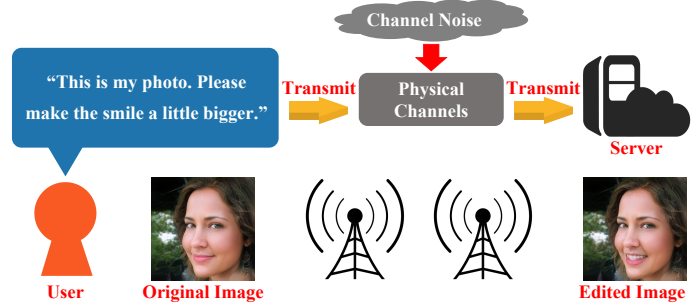


Fig. 1: Illustration of the dynamic semantic facial editing scenarios. During the transmission, users may wish to flexibly edit the original multimedia data according to their personal needs in a conversational and interactive way.

extracted semantic information from the original data, which should be encoded and transmitted with different importance. Reconstructing every part of the original data equally will undoubtedly waste the limited transmission bandwidth.

To alleviate this issue, the recently emerged semantic communications [6]–[14] (also known as task-oriented communications) only transmit the specific semantic information suitable for real-time CV tasks and exhibit a promising landscape to address this problem. By bridging the gap between bit-level transmission and task-oriented requirements, semantic communications can exploit much more of the scarce bandwidth to transmit task-related information, thus realizing better real-time CV tasks execution performance. On the other hand, Semantic Facial Editing [15]–[20], which stands out as one of the most important real-time CV tasks for user interaction and personalization, encounters various communication challenges when promoting its real-world deployment. As shown in Fig. 1, in many famous social platforms (e.g., Facebook, Instagram), before transmitting their own photos to the remote servers, users may wish to flexibly edit the original data according to their personal needs, such as adding smile to a face or altering the transparency of eyeglasses. Furthermore, such personal requirements can be fulfilled by providing dialogues to enable a more conversational and interactive experience. A crucial question still remains largely unexplored in existing works: *How to better transmit the facial semantics while also dynamically editing them according to the users’ needs?*

In this paper, we fill this research gap by proposing Editable-DeepSC, a novel cross-modal semantic communication approach for facial editing. Editable-DeepSC takes cross-modal text-image pairs as the inputs and transmits the edited semantic information of facial images based on textual instructions.

Part of this work [1] was presented in the IEEE 99th Vehicular Technology Conference (VTC2024-Spring), Singapore, June 2024.

Bin Chen is with the School of Computer Science and Technology, Harbin Institute of Technology, Shenzhen, Guangdong 518055, China (e-mail: chenbin2021@hit.edu.cn).

Wenbo Yu, Qinshan Zhang, and Shu-Tao Xia are with the Tsinghua Shenzhen International Graduate School, Tsinghua University, Shenzhen, Guangdong 518055, China (e-mail: wenbo.research@gmail.com; zhangqs24@mails.tsinghua.edu.cn; xiast@sz.tsinghua.edu.cn).

For such dynamic facial editing and communication scenarios, Editable-DeepSC faces the following challenges:

- $Q_1$ : *How to better compress the original data, so that satisfying editing effects can be achieved with less transmission bandwidth consumption?*
- $Q_2$ : *How to better realize a trade-off between editing effects and fidelity, so that targeted semantics are edited while other untargeted semantics still remain unaffected?*
- $Q_3$ : *How to better tackle the dynamically varying channel noise conditions, so that the model can generalize well to different circumstances of communication capabilities?*

To address the above challenges, we first theoretically discuss different transmission schemes that separately handle communications and editings, where both the cases of editings conducted at the receiver side (i.e., editings after the channel transfer) and editings conducted at the transmitter side (i.e., editings before the channel transfer) are taken into consideration. We find that by separately dealing with communications and editings, these schemes actually introduce more encoding and decoding steps, increase the data processing procedures, and are more likely to lose semantic mutual information, which will undermine the communication efficiency and eventually reduce the quality of edited images at the receiver side. In light of this, we emphasize the necessity to integrate editings into the communication chain, jointly optimize these two aspects, and minimize the data processing procedures to preserve more semantic mutual information.

Then, we propose semantic coding based on Generative Adversarial Networks (GAN) inversion methods [21]–[25]. By leveraging the abundant generative priors within the pre-trained StyleGAN [26], we encode the input images into the GAN latent space and map them to low-dimensional representations. Thus, we compactly represent the high-dimensional input data and considerably decrease the Channel Bandwidth Ratio (CBR) required to transmit the edited facial semantics. This addresses the aforementioned  $Q_1$ .

Inspired by the fact that DeepJSCC [27] combines source coding and channel coding to jointly optimize data compression and error correction, we propose Joint Editing-Channel Coding (JECC) based on iterative attributes matching. We design the JECC codecs by Fully Connected Layers, which iteratively exert minor modifications on the previous results of semantic coding to realize semantic editing and channel coding at the same time. Specifically, the current degrees of image attributes output by the pre-trained attribute predictor are compared with expected degrees after each iteration of modification to ensure fine-grained editings, where only the targeted attributes (e.g., bangs, eyeglasses) are edited without influencing other untargeted attributes. Moreover, the JECC codecs are trained through noisy channels to guarantee their basic robustness against channel noises in addition to the semantic editing abilities. Thus, we preserve more semantic mutual information due to the reduced data processing procedures of JECC and precisely perform fine-grained editings only on the targeted semantics. This addresses the aforementioned  $Q_2$ .

Benefiting from the recent successful applications of transfer learning techniques [28], [29], we propose SNR-aware channel coding based on model fine-tuning. Specifically, we

add two lightweight trainable adapters that do not change the shapes of inputs and outputs within the JECC codecs. When fine-tuning the models, only the parameters of these two adapters are adjusted to capture the distribution of new noise conditions. Meanwhile, the rest of the parameters are frozen to avoid forgetting the previously learned priors because of the fine-tuning. Thus, we efficiently adapt the model to the varying circumstances of communication capabilities by fine-tuning only a very small portion of the total parameters. This addresses the aforementioned  $Q_3$ .

To verify the effectiveness of our method, we conduct extensive experiments under various levels of SNRs and compare Editable-DeepSC with the baselines that separately handle communications and editings, where both editings after the channel transfer and before the channel transfer are evaluated. We also consider more rigorous and realistic simulation settings where the transmitter side users may hold high-resolution images or out-of-distribution (OOD) images. Numerous results indicate that Editable-DeepSC can achieve superior editing effects compared to the baseline methods while significantly saving the transmission bandwidth. For instance, in high-resolution settings, Editable-DeepSC only consumes less than 2% of the baseline methods' CBR, but still achieves the best editing performance both quantitatively and qualitatively. Furthermore, in the fine-tuning stage, Editable-DeepSC only adjusts 2.65% of the total parameters, but still considerably improves the editing effects under low SNRs and protect the edited semantics from channel noise corruptions.

To the best of our knowledge, we are the first to systematically and comprehensively investigate the communication problems of dynamic facial editing in this research field. Our main contributions are as follows:

- We theoretically analyze different transmission schemes that separately handle communications and editings. We discover that they actually increase the data processing procedures and are more likely to lose semantic mutual information. In light of this, we emphasize the necessity to integrate editings into the communication chain, jointly optimize these two aspects, and preserve more semantic mutual information.
- We propose semantic coding via GAN inversion. By leveraging the abundant generative priors within the pre-trained StyleGAN, we compactly compress the high-dimensional input images to low-dimensional representations to better reduce the bandwidth consumption.
- We propose Joint Editing-Channel Coding (JECC) via iterative attributes matching. We iteratively exert minor modifications on the results of semantic coding to reduce the data processing procedures for semantic mutual information preservation and precisely perform fine-grained editings only on the targeted semantics.
- We propose SNR-aware channel coding via model fine-tuning. We introduce two lightweight trainable adapters to capture the distribution of new noise conditions and freezes the rest parameters to avoid forgetting the priors, which helps the model generalize well to the varying circumstances of communication capabilities.
- Extensive experimental results demonstrate that Editable-

DeepSC can achieve superior performance compared to existing methods in terms of editing effects and transmission efficiency, even under more practical settings with high-resolution and out-of-distribution (OOD) images.

The rest of this paper is organized as follows. Section II illustrates the related works. Section III introduces the system model. Section IV elaborates on the implementation of Editable-DeepSC. Section V provides the experiment results. Section VI concludes this work.

## II. RELATED WORKS

### A. Semantic Facial Editing

Semantic Facial Editing aims to provide personalized facial manipulations specified by the users, and has emerged as one of the most important real-time CV tasks for its wide range of applications, including virtual content creation [30], augmented reality (AR) [31], and online conferencing [32]. This technology enables users to make intuitive edits to facial attributes such as expression, age, hairstyle, offering both creative flexibility and enhanced user experiences.

In the early stage of this research field’s development, many methods [15]–[17] focus on editing specific attributes, and rely heavily on extra manually provided knowledge such as landmarks. Recently, latent space based facial editing methods [18]–[20] are proposed due to the advancement of generative models like StyleGAN [26]. These methods typically strive to find semantically meaningful directions in the latent space of pre-trained generative models [33]–[38], so that shifting along the latent space would be able to achieve the desired editing in the vision space. InterFaceGAN [18] finds a hyperplane in the latent space to disentangle the facial semantics, and uses the normal vector of the hyperplane as the editing direction. Zhuang *et al.* [19] proposed to learn a mapping network to generate identity-specific directions within the latent space. However, both two methods [18], [19] neglect language guidance and lack conversational interaction. To alleviate this issue, Jiang *et al.* [20] proposed the SOTA method Talk2Edit, which enables customized editings via human language feedback.

### B. Task-Oriented Semantic Communications

Semantic communications prioritize the transmission of task-related semantic information rather than the original data with enhanced communication efficiency, and have showed great potential across various real-time CV tasks.

**Single-modal real-time image tasks.** Zhang *et al.* [6] proposed a DNN-based image semantic communication system, which only transmits the gradients back to the transmitter during training to protect the receiver’s privacy of downstream tasks. From the perspective of Reinforcement Learning (RL) [39], Huang *et al.* [7] adopted an adaptive semantic coding approach with an RL-based bit allocation model for better semantic similarity and image perception. Dong *et al.* [8] proposed the concept of semantic slice models, which can flexibly adapt the models to different requirements of model performance, channel situations and transmission goals.

**Single-modal real-time video tasks.** Tung *et al.* [9] first proposed to directly map video signals to channel symbols,

and utilized RL [39] to optimize the allocation of bandwidth among video frames. Jiang *et al.* [10] proposed a video semantic coding network based on keypoints transmission, and considerably reduced resources consumption without losing the main details. Wang *et al.* [11] exploited nonlinear transform and conditional coding architecture to adaptively extract semantic features across video frames, and surpassed traditional wireless video coded transmission schemes.

**Multi-modal real-time CV tasks.** Xie *et al.* [12] proposed a multi-modal semantic communication system for Visual Question Answering (VQA) tasks, which utilizes MAC networks [40] to deal with the interconnected cross-modal data and generate the answers to VQA tasks. Xie *et al.* [13] further considered the multi-modal multi-user transmission scenarios and proposed a unified framework to effectively reduce the mutual interference between different users. Wang *et al.* [14] utilized Transformer [41] to design a distributed Audio-Visual Parsing (AVP) network under transmission scenarios with superior multi-modal parsing performance.

However, to the best of our knowledge, the cross-modal semantic communication challenges under dynamic facial editing scenarios have not yet been systematically explored up to now. In this paper, we aim to fill this research gap and comprehensively address these problems.

## III. SYSTEM MODEL

As shown in Fig. 2, our proposed Editable-DeepSC mainly consists of the Text Semantic Encoder, the Image Semantic Encoder, the Joint Editing-Channel Encoder, and the Joint Semantic-Channel Decoder, where channel noise corruptions from the real world are also taken into consideration.

### A. Semantic Transmitter

The input image  $S_I$  is first transformed by the Image Semantic Encoder into low-dimensional representations for data compression, i.e.,

$$E_I = \mathcal{SE}_{\mathcal{I}}(S_I; \alpha), \quad (1)$$

where  $\mathcal{SE}_{\mathcal{I}}(\cdot; \alpha)$  denotes the Image Semantic Encoder with the parameters  $\alpha$ . Similarly, the corresponding instructive sentence  $S_T$  is also encoded by the Text Semantic Encoder  $\mathcal{SE}_{\mathcal{T}}(\cdot; \beta)$  with the parameters  $\beta$  to acquire the textual semantic information, which is highly relevant to the anticipated editing:

$$E_T = \mathcal{SE}_{\mathcal{T}}(S_T; \beta). \quad (2)$$

Next,  $E_I$  and  $E_T$  are sent into the Joint Editing-Channel Encoder  $\mathcal{JECCE}(\cdot, \cdot; \gamma)$  with the parameters  $\gamma$ , which will apply semantic editing as well as channel coding to the transmitted information in the meantime:

$$X = \mathcal{JECCE}(E_I, E_T; \gamma). \quad (3)$$

The output of  $\mathcal{JECCE}(\cdot, \cdot; \gamma)$ , i.e.,  $X$ , is then transmitted through the physical channels. We enforce an average transmission power constraint on  $X$  to ensure that it does not exceed the limits of current communication capabilities:

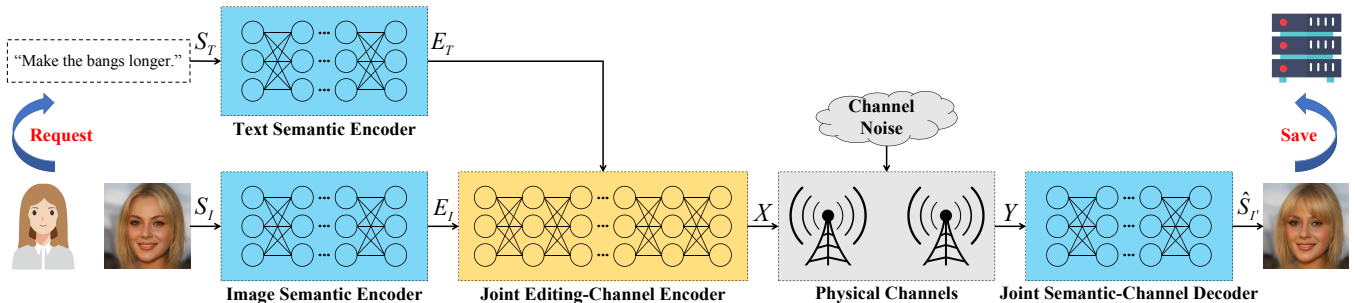


Fig. 2: Overview of the proposed framework. Editable-DeepSC mainly consists of the Text Semantic Encoder, the Image Semantic Encoder, the Joint Editing-Channel Encoder, and the Joint Semantic-Channel Decoder, where channel noise corruptions from the real world are also taken into consideration.

$$\frac{1}{k} \cdot \|X\|_2^2 \leq P, \quad (4)$$

where  $k$  is the length of  $X$  and  $P$  is the power constraint.

Following the previous works [42]–[44] in this research field, the Channel Bandwidth Ratio (CBR) can be defined as:

$$\rho = \frac{k}{H \times W \times C}, \quad (5)$$

where  $H$ ,  $W$ , and  $C$  represent the image’s height, width, and color channels. Smaller  $\rho$  indicates better compression.

### B. Semantic Receiver

The transmitted signals are usually corrupted by the channel noise. Consequently, only the disrupted forms of the edited semantic information can be detected at the receiver side, i.e.,

$$Y = h * X + N, \quad (6)$$

where  $Y$  represents the received edited semantic information,  $h$  denotes the channel coefficients, and  $N$  denotes the Gaussian noise, whose elements are independent of each other and have the same mean and variance.

Finally,  $Y$  is mapped back to the high-dimensional vision domain to get the edited image required by the transmitter:

$$\hat{S}'_I = \mathcal{JSCD}(Y; \theta), \quad (7)$$

where  $\mathcal{JSCD}(\cdot; \theta)$  indicates the Joint Semantic-Channel Decoder with the parameters  $\theta$ . Note that  $\mathcal{JSCD}(\cdot; \theta)$  will apply semantic decoding as well as channel decoding to  $Y$  at the same time, which will reduce the semantic errors caused by the channel noise. Moreover, since only the edited images are ultimately required and there is no need to reconstruct the instructive sentences, the Text Semantic Decoder is unnecessary in our model and thus not considered.

### C. Theoretical Rationality

To justify the rationality of our proposed Editable-DeepSC, we consider the alternative separate schemes below and theoretically demonstrate the superiority of our approach. Specifically, based on the sequence of communications and editings, we consider the following separate schemes:

$M_1$ : (editings after the channel transfer) The transmitter sends the images, and then the receiver edits them.

$M_2$ : (editings before the channel transfer) The transmitter edits the images, and then sends them to the receiver.

For the encoding and decoding steps of DNN as well as the channel transfer steps, the outputs of each stage are largely dependent on the current inputs instead of the previous outputs, which approximately satisfies the Markov property. Thus, as suggested in many previous works [45], [46], we approximate the above encoding, decoding, and channel transfer steps as a successive Markov chain  $K_0 \rightarrow K_1 \rightarrow \dots \rightarrow K_n$ , where  $K_0$  indicates the distribution of original images at the transmitter side,  $n$  is the total number of data processing procedures,  $K_n$  indicates the distribution of ultimate edited images at the receiver side, and  $K_s$  ( $0 < s < n$ ) indicates the distribution of a series of intermediate representations during the above steps. For any two continuous transitions  $U \rightarrow V \rightarrow W$  from the whole Markov chain, we have the Data Processing Inequality (DPI) [47] as shown in Theorem 1.

**Theorem 1. (Data Processing Inequality)** If  $U \rightarrow V \rightarrow W$ , then  $\mathcal{I}(U; V) \geq \mathcal{I}(U; W)$ .

*Proof.* See Appendix A.

By applying DPI to the whole Markov chain  $K_0 \rightarrow K_1 \rightarrow \dots \rightarrow K_n$  as pointed out in [45], we have  $\mathcal{I}(K_0; K_1) \geq \mathcal{I}(K_0; K_2) \geq \dots \geq \mathcal{I}(K_0; K_n)$ . This implies that as the data processing procedures increase, the semantic mutual information about the original distribution  $K_0$  carried by the intermediate distribution  $K_s$  will decrease and cannot be recovered in the subsequent steps. Therefore, the aforementioned separate schemes  $M_1$  and  $M_2$  that have more encoding and decoding steps are more likely to lose semantic mutual information, which will eventually limit the perceptual performance of edited images. On the contrary, Editable-DeepSC integrates editings into the communication chain to decrease the data processing procedures, and will thus preserve more semantic mutual information with enhanced tasks execution performance.

## IV. METHOD

### A. Semantic Coding via Pre-trained GAN Inversion

We leverage the GAN inversion methods based on Style-GAN [26] priors to design the Image Semantic Encoder

$\mathcal{SE}_{\mathcal{I}}(\cdot; \alpha)$ , as there is rich prior knowledge within the pre-trained GAN to reduce the representation dimension. To be specific, given an input image  $S_I$ , a random vector  $z$  is first initialized in the StyleGAN latent space. The random vector  $z$  is then fed into the pre-trained StyleGAN Generator  $G(\cdot)$  to generate an initial image  $I_g = G(z)$ . The distortion  $J(z)$  between  $S_I$  and  $I_g$  is calculated as:

$$J(z) = \lambda_{inv} \cdot MSE(S_I, I_g) + LPIPS(S_I, I_g). \quad (8)$$

The distortion  $J(z)$  is measured from both the pixel level and the perceptual level, balanced by the hyper-parameter  $\lambda_{inv}$ . In this paper, we adopt the MSE loss for the pixel level distortion and the LPIPS loss [48] for the perceptual level distortion. To obtain the latent vector that perfectly suits the original image, we can minimize  $J(z)$  and update  $z$  by iteratively performing the gradient descent until convergence:

$$z^{(t)} = z^{(t-1)} - \eta_{inv} \cdot \nabla_{z^{(t-1)}} J(z^{(t-1)}), \quad (9)$$

where  $r_{inv}$  is the number of total inversion iterations,  $z^{(0)}$  denotes the randomly initialized latent vector,  $z^{(t)}$  ( $1 \leq t \leq r_{inv}$ ) denotes the outcome after the  $t$ -th iteration, and  $\eta_{inv}$  is the inversion learning rate. Upon completing the optimization of (9), we will obtain the output of semantic coding, which is denoted as  $E_I = z^{(r_{inv})}$ . Note that the dimension of  $z$  is often much smaller than the dimension of  $S_I$ , hence we can greatly compress the original data and reduce the channel bandwidth ratio (CBR) defined in (5).

As for the Joint Semantic-Channel Decoder  $\mathcal{JSCD}(\cdot; \theta)$ , we first send  $Y$  to another pre-trained StyleGAN Generator for semantic decoding to map the compressed data back to high-dimensional images. Besides, we additionally introduce lightweight trainable parameters for channel decoding to reduce the semantic errors caused by the channel noise, which we will detailedly discuss in Section IV-C.

### B. Joint Editing-Channel Coding via Attributes Matching

**Editing Attributes.** Firstly, we need to quantitatively measure the attributes for editing (e.g., bangs, eyeglasses). We introduce an attribute predictor  $P(\cdot)$  pre-trained on the CelebA-Dialog dataset [49], which consists of detailed manual annotations regarding the attributes of each training image. We send the original image to  $P(\cdot)$  and obtain its output  $\{a_1, a_2, \dots, a_i, \dots, a_m\}$ , where the value of  $a_i$  indicates the degree of each attribute (e.g., the length of the bangs, the transparency of eyeglasses),  $m$  is the total number of attributes, and  $u$  is the same maximum degree value for each attribute.

**Editing Semantic Information Extraction.** We utilize the Long Short-Term Memory (LSTM) [50] network to implement the Text Semantic Encoder  $\mathcal{SE}_{\mathcal{T}}(\cdot; \beta)$ , which can capture the dependencies between various parts of the input texts. We train  $\mathcal{SE}_{\mathcal{T}}(\cdot; \beta)$  on the CelebA-Dialog dataset [49] using the cross-entropy loss, where the training texts are manually annotated with their actual semantic information (i.e., the index of targeted attribute  $i_{tar} \in \{1, 2, \dots, m\}$ , the direction of editing  $d_{tar} \in \{-1, +1\}$ , and the degree of modification  $\Delta_{tar} \in \{0, 1, \dots, u\}$ ) as the labels. In the test time, the

original texts are tokenized into words or subwords according to the dictionary and then sent to  $\mathcal{SE}_{\mathcal{T}}(\cdot; \beta)$ . The ultimate text encodings  $E_T$  will contain the aforementioned semantic information needed for editing:  $i_{tar}$ ,  $d_{tar}$  and  $\Delta_{tar}$ .

**Joint Editing-Channel Coding (JECC).** Inspired by the fact that DeepJSCC [27] combines source coding and channel coding to jointly optimize data compression and error correction, we implement the Joint Editing-Channel Encoder  $\mathcal{JECCE}(\cdot, \cdot; \gamma)$  by Fully Connected Layers  $\mathcal{M}(\cdot; \gamma)$  to jointly optimize editings and communications for reduced data processing procedures. Note that  $\mathcal{M}(\cdot; \gamma)$  only takes  $E_I$  as the input, while  $E_T$ , the other input of  $\mathcal{JECCE}(\cdot, \cdot; \gamma)$ , is utilized to obtain  $i_{tar}$ ,  $d_{tar}$  and  $\Delta_{tar}$  that guide the semantic editing. In the test time, we first compute the expected degree of targeted attribute by  $\{a_1, a_2, \dots, a_i, \dots, a_m\}$ ,  $i_{tar}$ ,  $d_{tar}$ , and  $\Delta_{tar}$ :

$$a_{exp} = \min(\max(a_{i_{tar}} + \Delta_{tar} \cdot d_{tar}, 0), u), \quad (10)$$

where the minimum function  $\min(\cdot, \cdot)$  and the maximum function  $\max(\cdot, \cdot)$  are adopted to ensure that  $0 \leq a_{exp} \leq u$ . Then, we iteratively exert minor modifications on  $E_I$ :

$$E_{I'}^{(t)} = E_{I'}^{(t-1)} + d_{tar} \cdot \mathcal{M}(E_{I'}^{(t-1)}; \gamma), \quad (11)$$

where  $r_{edit}$  is the maximum number of total editing iterations,  $E_{I'}^{(0)}$  is the same as  $E_I$ , and  $E_{I'}^{(t)}$  ( $1 \leq t \leq r_{edit}$ ) denotes the outcome after the  $t$ -th iteration. After each iteration of modification,  $E_{I'}^{(t)}$  is delivered to the StyleGAN Generator  $G(\cdot)$  to reconstruct an intermediate image, which will be sent to the pre-trained attribute predictor  $P(\cdot)$  in to check whether the anticipated requirement is satisfied. The predicted degree of the intermediate image calculated by  $P(\cdot)$  will be compared with the expected degree  $a_{exp}$ . Once they match with each other, the iteration will stop and  $E_{I'}^{(t)}$  will be regarded as the output of  $\mathcal{JECCE}(\cdot, \cdot; \gamma)$ . Otherwise,  $\mathcal{M}(\cdot; \gamma)$  will continue to iteratively make small movements on  $E_{I'}^{(t)}$  until the target is reached or the maximum number  $r_{edit}$  is exceeded.

**Training Strategy of the JECC Codecs.** To train  $\mathcal{M}(\cdot; \gamma)$  for the  $i$ -th attribute, we set the expected degree of the  $i$ -th attribute to be  $(a_i + 1)$  so that the model can learn how to perform fine-grained editings on each attribute. Note that the situation for  $(a_i - 1)$  is completely symmetrical when  $d_{tar}$  is set to  $-1$ . The predictor loss  $\mathcal{L}_{pred}$  can be calculated by adopting the cross-entropy loss:

$$\mathcal{L}_{pred} = - \sum_{i=1}^m \sum_{j=0}^u b_{ij} \cdot \log(p_{ij}), \quad (12)$$

where  $b_{ij} \in \{0, 1\}$  is the one-hot representation of the expected attribute degrees, and  $p_{ij}$  is the output of the pre-trained attribute predictor  $P(\cdot)$  on the edited image. We also leverage the identity preservation loss  $\mathcal{L}_{id}$  to better keep the original facial identity. We use ready-made facial recognition model to extract the features. The extracted features for facial recognition should be as similar as possible:

$$\mathcal{L}_{id} = \|F(I_a) - F(I_b)\|_1, \quad (13)$$

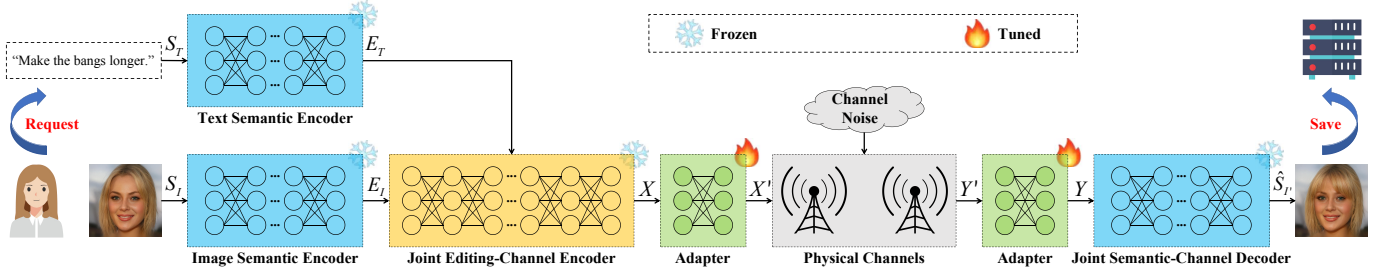


Fig. 3: Illustration of our SNR-aware channel coding based on model fine-tuning. We introduce two lightweight trainable adapters that do not change the shapes of inputs and outputs to the Joint Editing-Channel Encoder and the Joint Semantic-Channel Decoder. When fine-tuning the models, only the parameters of these two adapters are adjusted to capture the distribution of new noise conditions, and the rest parameters are frozen to avoid forgetting the previously learned priors from Section IV-B.

where  $I_a, I_b$  are the images after and before the editing, and  $F(\cdot)$  is the pre-trained face recognition model [51]. The discriminator loss  $\mathcal{L}_{disc}$  is also adopted to ensure the fidelity on the generated images:

$$\mathcal{L}_{disc} = -D(I_a), \quad (14)$$

where  $D(\cdot)$  is the output of the pre-trained StyleGAN [26] discriminator. Finally, the total loss can be calculated as:

$$\mathcal{L} = \lambda_{pred} \cdot \mathcal{L}_{pred} + \lambda_{id} \cdot \mathcal{L}_{id} + \lambda_{disc} \cdot \mathcal{L}_{disc}, \quad (15)$$

where  $\lambda_{pred}$ ,  $\lambda_{id}$ , and  $\lambda_{disc}$  are the weight factors. We utilize the total loss  $\mathcal{L}$  to train  $\mathcal{M}(\cdot; \gamma)$  through the noisy channels under high SNRs to guarantee their basic robustness against channel noises in addition to the semantic editing abilities. In our preliminary experiments, we find that if the training SNRs are low, the editing effects are not satisfying because the extreme channel noises will instead disrupt the learning of semantic editing. Therefore, we train  $\mathcal{M}(\cdot; \gamma)$  only under high SNRs and discuss how to fine-tune the JECC codecs under all levels of SNRs in Section IV-C.

### C. SNR-aware Channel Coding via Model Fine-tuning

As shown in Fig. 3, we introduce two lightweight trainable adapters that consist of Fully Connected Layers and do not change the shapes of inputs and outputs to the Joint Editing-Channel Encoder  $\mathcal{JEC}(\cdot, \cdot; \gamma)$  and the Joint Semantic-Channel Decoder  $\mathcal{JSCD}(\cdot; \theta)$ . The output of  $\mathcal{M}(\cdot; \gamma)$  is sent to the Channel Encoder Adapter  $\mathcal{A}_{CE}(\cdot; \phi)$  to obtain the final outcome of channel encoding:

$$X' = \mathcal{A}_{CE}(X; \phi). \quad (16)$$

$X'$  is then transmitted through the physical channels obeying the similar procedure described in (6) and the receiver will obtain  $Y'$ . Then,  $Y'$  is sent to the Channel Decoder Adapter  $\mathcal{A}_{CD}(\cdot; \psi)$  to acquire the new input of  $\mathcal{JSCD}(\cdot; \theta)$ :

$$Y = \mathcal{A}_{CD}(Y'; \psi). \quad (17)$$

In the fine-tuning stage, we randomly select  $n_{ft}$  images that strictly have no intersections with the images used in the test time. For each new SNR level that needs to be adapted to, we transmit the fine-tuning images following the procedures

defined in Section III as well as (16) and (17). We compute the LPIPS loss [48] between the final received image  $\hat{S}_I'$  and the original image  $S_I$  to measure the perceptual distortion for the fine-tuning loss  $\mathcal{L}_{ft}$ . We update the parameters of  $\mathcal{A}_{CE}(\cdot; \phi)$  and  $\mathcal{A}_{CD}(\cdot; \psi)$  using the gradient descent:

$$\begin{cases} \phi^{(t)} = \phi^{(t-1)} - \eta_{ft} \cdot \nabla_{\phi^{(t-1)}} \mathcal{L}_{ft} \\ \psi^{(t)} = \psi^{(t-1)} - \eta_{ft} \cdot \nabla_{\psi^{(t-1)}} \mathcal{L}_{ft}, \end{cases} \quad (18)$$

where  $r_{ft}$  is the number of total fine-tuning iterations,  $\phi^{(t)}, \psi^{(t)}$  ( $1 \leq t \leq r_{ft}$ ) are the results after the  $t$ -th iteration, and  $\eta_{ft}$  is the fine-tuning learning rate. When the fine-tuning is completed, these two adapters can capture the data distribution of current SNR level and enhance the perceptual quality of edited images in the test time, especially under extreme channel conditions. And the rest parameters are frozen to avoid forgetting the previously learned priors from Section IV-B.

## V. EXPERIMENTS

### A. Experiment Setup

**Simulation Datasets.** As for the textual instruction  $S_T$ , we use the editing requests from the CelebA-Dialog dataset [49] for all the experiments. As for the original image  $S_I$ : (1) In the main experiments, we consider relatively simple scenarios and choose from the CelebA dataset [52], whose images are cropped to the resolution of  $128 \times 128$  and have similar distribution with the training set of StyleGAN [26]; (2) In the more realistic high-resolution experiments, we choose from the CelebA-HQ dataset [53] with the resolution of  $1024 \times 1024$ ; (3) In the more realistic out-of-distribution (OOD) experiments, we choose from the MetFaces dataset [54] with the resolution of  $128 \times 128$ , whose facial images are from artworks and have an inherent distribution bias with the natural facial images of StyleGAN training set. As for the fine-tuning images, we use images from the CelebA dataset [52] for the resolution of  $128 \times 128$ , and use images from the CelebA-HQ dataset [53] for the resolution of  $1024 \times 1024$ . We strictly ensure that the fine-tuning images are few in number ( $n_{ft} < 20$ ) and have no intersections with the images used in the test time.

**Evaluation Baselines.** To the best of our knowledge, there exists no other semantic communication approach tailored for cross-modal facial editing tasks by now. Therefore, we

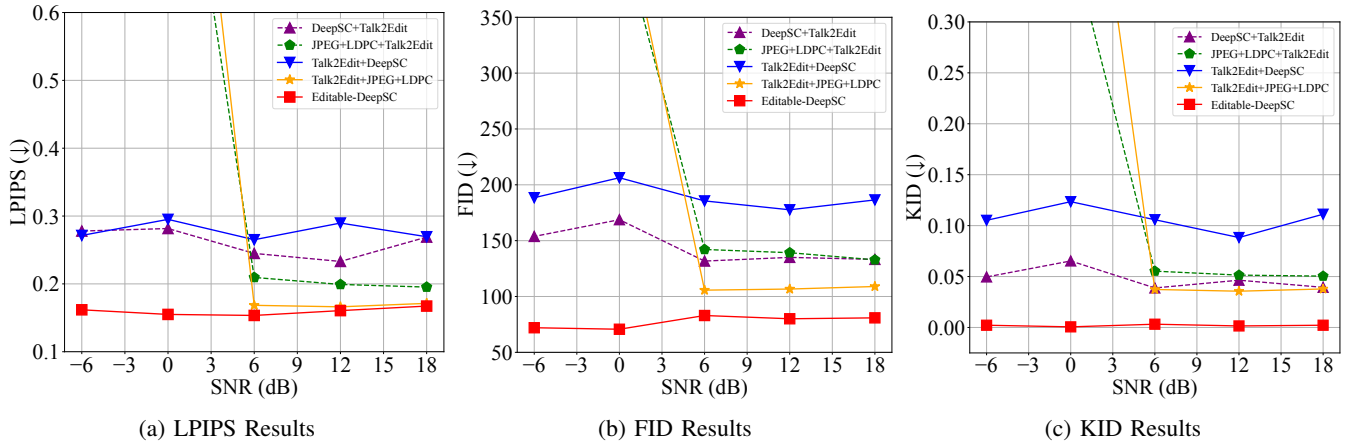


Fig. 4: Quantitative comparison of different methods on the CelebA dataset (resolution  $128 \times 128$ ) for cross-modal language-driven image editing and transmission tasks. Note that  $\downarrow$  indicates that the lower the metric, the better the performance.

compare Editable-DeepSC with the classical traditional communication methods JPEG [55] and LDPC [56], the novel single-modal image semantic communication method DeepSC [6], and the SOTA text-driven image editing method Talk2Edit [20] in the Computer Vision (CV) field. We rearrange these methods and consider the following baselines that separately handle communications and editings:

- **DeepSC+Talk2Edit.** DeepSC [6] is utilized to send  $S_I$  from the transmitter to the receiver. And the transmission of  $S_T$  is assumed to be error-free, which means that the received sentences are identical to the original ones to enhance the capabilities of this baseline for better persuasiveness. Then, Talk2Edit [20] is utilized to perform the text-driven image editing at the receiver side. This consists with the scheme  $M_1$  mentioned in Section III-C.
- **JPEG+LDPC+Talk2Edit.** JPEG [55] is utilized for image source coding and LDPC [56] is utilized for image channel coding to send  $S_I$  from the transmitter to the receiver. And the transmission of  $S_T$  is also assumed to be error-free. Then, Talk2Edit [20] is utilized to perform the text-driven image editing at the receiver side. This consists with the scheme  $M_1$  mentioned in Section III-C.
- **Talk2Edit+DeepSC.** Talk2Edit [20] is utilized to perform the text-driven image editing at the transmitter side. Then, DeepSC [6] is utilized to send the edited images from the transmitter to the receiver. This consists with the scheme  $M_2$  mentioned in Section III-C.
- **Talk2Edit+JPEG+LDPC.** Talk2Edit [20] is utilized to perform the text-driven image editing at the transmitter side. Then, JPEG [55] is utilized for image source coding and LDPC [56] is utilized for image channel coding to send the edited images from the transmitter to the receiver. This consists with the scheme  $M_2$  mentioned in Section III-C.

**Quantitative Metrics.** To quantitatively measure the editing effects of different methods, we adopt LPIPS [48], FID [57], and KID [58]. LPIPS utilizes pre-trained convolutional networks to extract the features of original images and edited images to calculate the perceptual differences. FID and KID

computes the distribution differences between the original images and edited images. Smaller LPIPS, FID, and KID scores indicate better editing effects. To quantitatively measure the communication efficiency of different methods, we adopt the Channel Bandwidth Ratio (CBR) defined in (5). Smaller CBR indicates better compression and communication efficiency.

**Implementation Details.** To simulate the varying communication circumstances, we set the SNR levels of  $-6$  dB,  $0$  dB,  $6$  dB,  $12$  dB,  $18$  dB for all the methods. For Editable-DeepSC,  $\lambda_{inv}$ ,  $\eta_{inv}$ ,  $r_{inv}$ ,  $\eta_{ft}$ , and  $n_{ft}$  are set as  $1.0$ ,  $0.10$ ,  $110$ ,  $1 \times 10^{-4}$ , and  $10$ , respectively. For DeepSC [6], the learning rate is  $1 \times 10^{-3}$  and the batch size is  $4$ . For JPEG [55] and LDPC [56], the target bpp under the resolution of  $128 \times 128$  is  $0.7$ , the target bpp under the resolution of  $1024 \times 1024$  is  $0.2$ , and the QAM order is  $4$ . For Talk2Edit [20], we adopt its official code implementation. All the experiments are conducted on NVIDIA GeForce RTX 2080 Ti GPUs.

## B. Main Results

We compare Editable-DeepSC with the baselines on the CelebA dataset. From Fig. 4, we find that Editable-DeepSC realizes the best results in terms of LPIPS, FID, and KID with significant improvements. For instance, when the SNR level is  $-6$  dB, the LPIPS, FID, and KID scores of Editable-DeepSC are improved by  $40.4\%$ ,  $53.2\%$ , and  $95.6\%$  than the second best method, respectively. These results indicate that Editable-DeepSC achieves excellent editing effects with high fidelity and quality, outperforming the baselines that separately handle communications and editings. We also observe that the performance of JPEG+LDPC+Talk2Edit and Talk2Edit+JPEG+LDPC will decrease rapidly when the SNR level is below  $6$  dB, which is consistent with the fact that the traditional communications suffer greatly from the *cliff effect*.

Fig. 5 illustrates the qualitative comparison of different methods at the noise level of  $6$  dB. We notice that Editable-DeepSC indeed achieves the best visualization results. Although the other baselines also manage to edit the images, their effects are not as vivid and natural as those achieved with Editable-DeepSC. This is because Editable-DeepSC reduces



DeepSC+Talk2Edit   JPEG+LDPC+Talk2Edit   Talk2Edit+DeepSC   Talk2Edit+JPEG+LDPC   Editable-DeepSC   Original

Fig. 5: Qualitative comparison of different methods on the CelebA dataset (resolution  $128 \times 128$ ) for cross-modal language-driven image editing and transmission tasks at the SNR of 6 dB. The instructive sentences for the 1st and 2nd rows are respectively “I kind of want the smile to be less obvious” and “Smile more”.

TABLE I: Compression effectiveness of different methods with the resolution of  $128 \times 128$ , measured by the Channel Bandwidth Ratio (CBR) defined in (5).

Method	Resolution	CBR ( $\downarrow$ )
DeepSC+Talk2Edit	$128 \times 128$	0.0833
JPEG+LDPC+Talk2Edit	$128 \times 128$	0.0389
Talk2Edit+DeepSC	$128 \times 128$	0.0833
Talk2Edit+JPEG+LDPC	$128 \times 128$	0.0389
Editable-DeepSC	$128 \times 128$	<b>0.0104</b>

the data processing procedures and preserves more semantic mutual information, which eventually leads to more satisfying editing performance. Table I shows the compression effectiveness of different methods from the perspective of CBR defined in (5). We find that Editable-DeepSC only utilizes around 12.5% or 26.7% of the baselines’ CBR, yet it still achieves extraordinary editing effects and outperforms all the baselines. Editable-DeepSC not only performs high-quality editings, but

also considerably saves the transmission bandwidth.

### C. High-Resolution Scenario Results

We then consider more realistic settings where the image resolution is expanded to  $1024 \times 1024$  on the CelebA-HQ dataset. Fig. 6 presents the LPIPS, FID, and KID results while Table II presents the CBR results. The amplification of image pixels objectively increases the complexity of editing and transmission tasks. However, we conclude that Editable-DeepSC again achieves the best LPIPS and KID scores under almost all the tested cases. As for the FID scores, although Editable-DeepSC can’t obtain the best performance in some cases, it only uses around 0.2% or 1.8% of the baselines’ CBR with much lower bandwidth consumption as shown in Table II. In general, Editable-DeepSC still exhibits great robustness and efficiency under high-resolution scenarios.

Fig. 7 shows the visualization results on the CelebA-HQ dataset. We notice that Editable-DeepSC can acquire better editing effects than the other baselines, with fewer artifacts or

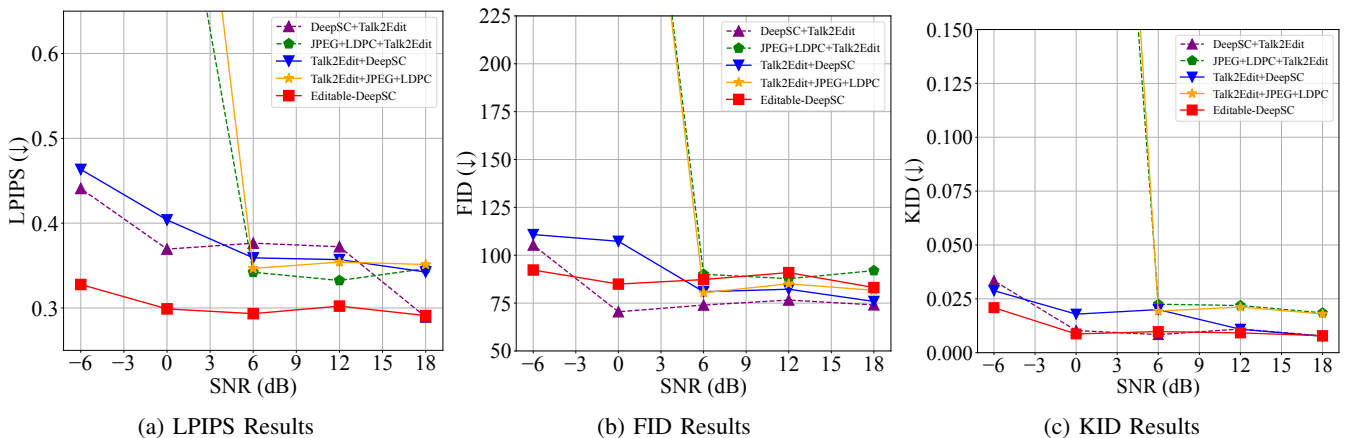


Fig. 6: Quantitative comparison of different methods on the CelebA-HQ dataset (resolution  $1024 \times 1024$ ) for cross-modal language-driven image editing and transmission tasks. Note that  $\downarrow$  indicates that the lower the metric, the better the performance.



DeepSC+Talk2Edit    JPEG+LDPC+Talk2Edit    Talk2Edit+DeepSC    Talk2Edit+JPEG+LDPC    Editable-DeepSC    Original

Fig. 7: Qualitative comparison of different methods on the CelebA-HQ dataset (resolution  $1024 \times 1024$ ) for cross-modal language-driven image editing and transmission tasks at the SNR of 6 dB. The instructive sentences for the 1st and 2nd rows are respectively “What about trying bangs that leaves half of the forehead visible” and “Make the face slightly younger”.

TABLE II: Compression effectiveness of different methods with the resolution of  $1024 \times 1024$ , measured by the Channel Bandwidth Ratio (CBR) defined in (5).

Method	Resolution	CBR ( $\downarrow$ )
DeepSC+Talk2Edit	$1024 \times 1024$	0.0833
JPEG+LDPC+Talk2Edit	$1024 \times 1024$	0.0111
Talk2Edit+DeepSC	$1024 \times 1024$	0.0833
Talk2Edit+JPEG+LDPC	$1024 \times 1024$	0.0111
Editable-DeepSC	$1024 \times 1024$	<b>0.0002</b>

blurs. In particular, for the 2nd row of images where the textual instruction is to make the face slightly younger, Editable-DeepSC manages to deal with this request in a fine-grained way and moderately alter the degree of youth. However, all the other baselines overly modify the original face to appear too immature and there is the problem of excessive editing. This again validates the necessity to integrate editings into the communication chain for reduced data processing procedures,

which can retain more semantic mutual information from the original images and precisely conduct fine-grained editings.

#### D. Out-Of-Distribution (OOD) Scenario Results

We also evaluate Editable-DeepSC and the other baselines under out-of-distribution (OOD) settings on the MetFaces dataset, where the distributions of training data and testing data are mismatched. From Fig. 8, we observe that Editable-DeepSC continuously obtains the best LPIPS, FID, and KID scores. These results prove that Editable-DeepSC possesses outstanding OOD generalizability, and is able to consistently surpass those baselines that separately communicate and edit even on unseen artistic datasets.

The visualization results in Fig. 9 further demonstrate that Editable-DeepSC can precisely edit the OOD images without influencing other unrelated regions. In contrast, all the other baselines struggle to realize the semantic editing while maintaining the fidelity, and encounter image quality degradation or even collapse under the more rigorous OOD scenarios. Our

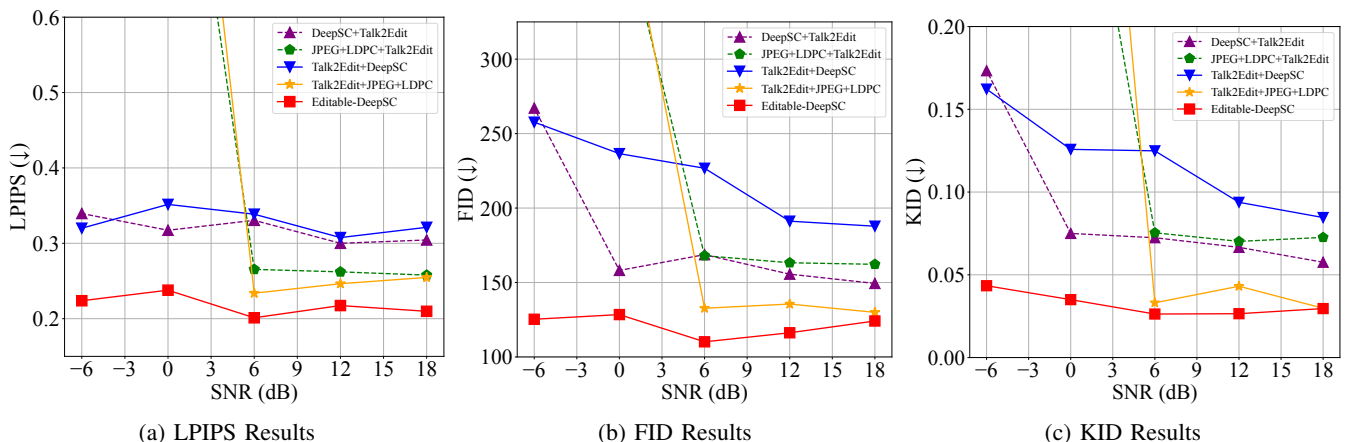


Fig. 8: Quantitative comparison of different methods on the MetFaces dataset (resolution  $128 \times 128$ ) for cross-modal language-driven image editing and transmission tasks. Note that  $\downarrow$  indicates that the lower the metric, the better the performance.



DeepSC+Talk2Edit    JPEG+LDPC+Talk2Edit    Talk2Edit+DeepSC    Talk2Edit+JPEG+LDPC    Editable-DeepSC    Original

Fig. 9: Qualitative comparison of different methods on the MetFaces dataset (resolution  $128 \times 128$ ) for cross-modal language-driven image editing and transmission tasks at the SNR of 18 dB. The instructive sentences for the 1st and 2nd rows are respectively “Make the bangs longer” and “What about trying extremely long fringe”.

TABLE III: Quantitative results under different values of  $r_{inv}$ . We also report the total time costs averaged over each image.

Metric	70	90	110	130	150
LPIPS ( $\downarrow$ )	0.1807	0.1695	<b>0.1618</b>	0.1649	0.1666
FID ( $\downarrow$ )	73.94	73.75	<b>72.03</b>	73.11	76.07
KID ( $\downarrow$ )	0.0045	0.0067	<b>0.0022</b>	0.0025	0.0050
Total Time ( $\downarrow$ )	<b>13.3s</b>	14.0s	14.6s	17.0s	17.7s

combination of editings and communications has indeed come into effect for better downstream tasks performance.

### E. Further Analysis

In this subsection, we provide deeper insights for our method, such as the influences of each proposed component. By default, *the experiments are conducted on the CelebA dataset with the same settings as Section V-B at the SNR of  $-6$  dB unless otherwise specified.*

**The influences of pre-trained GAN inversion.** First, we explore the impacts of the proposed GAN inversion based semantic coding by changing the number of total inversion iterations  $r_{inv}$ . From Table III, we notice that when  $r_{inv}$  is small, increasing its value indeed improves the editing performance as the GAN inversion is more fully optimized, which validates the contribution of this component. However, when  $r_{inv}$  is large, further increasing its value cannot improve the editing performance and will also introduce more time costs. Thus, our adoption of  $r_{inv} = 110$  is reasonable, for it strikes a better balance between editing effects and time costs.

**The influences of iterative attributes matching.** Next, we study the impacts of the iterative attributes matching mechanism by removing it from Editable-DeepSC. As shown in Fig. 10, when the iterative attributes matching mechanism is excluded, Editable-DeepSC will be unable to precisely perform the anticipated editings according to the given texts in a fine-grained way. This again provides evidence for the contribution of our iterative attributes matching mechanism.

TABLE IV: Quantitative results on whether the fine-tuning mechanism is incorporated into Editable-DeepSC.

Dataset	Method	LPIPS ( $\downarrow$ )	FID ( $\downarrow$ )	KID ( $\downarrow$ )
CelebA	w/o Fine-Tuning	0.3049	117.77	0.0404
	w/ Fine-Tuning	<b>0.1618</b>	<b>72.03</b>	<b>0.0022</b>
CelebA-HQ	w/o Fine-Tuning	0.4764	116.20	0.0307
	w/ Fine-Tuning	<b>0.3277</b>	<b>92.28</b>	<b>0.0209</b>
MetFaces	w/o Fine-Tuning	0.3622	182.44	0.1185
	w/ Fine-Tuning	<b>0.2238</b>	<b>125.33</b>	<b>0.0434</b>

TABLE V: Total time costs of different methods averaged over each image with the resolutions of  $128 \times 128$  and  $1024 \times 1024$ .

Method	$128 \times 128$	$1024 \times 1024$
DeepSC+Talk2Edit	34.1s	86.8s
JPEG+LDPC+Talk2Edit	33.2s	47.6s
Talk2Edit+DeepSC	32.6s	85.9s
Talk2Edit+JPEG+LDPC	32.8s	41.9s
Editable-DeepSC	<b>14.6s</b>	<b>39.1s</b>

**The influences of model fine-tuning.** Similarly, we also investigate the impacts of the model fine-tuning mechanism in Table IV and Fig. 11. We discover that under the extreme channel condition of  $-6$  dB SNR, the fine-tuning mechanism plays a crucial role in preserving the quality and fidelity of edited images, while removing it will conversely generate unnatural or even collapsed regions. These results also verify the contribution of our fine-tuning mechanism.

**Computational costs.** Next, we provide analysis on computational costs. From Table V, Editable-DeepSC has the smallest total time costs and surpasses all the baselines. This is because Editable-DeepSC jointly optimizes the communications and editings with reduced data processing procedures, while the separate baselines repeatedly encode the data and result in low efficiency. Furthermore, Editable-DeepSC consumes less

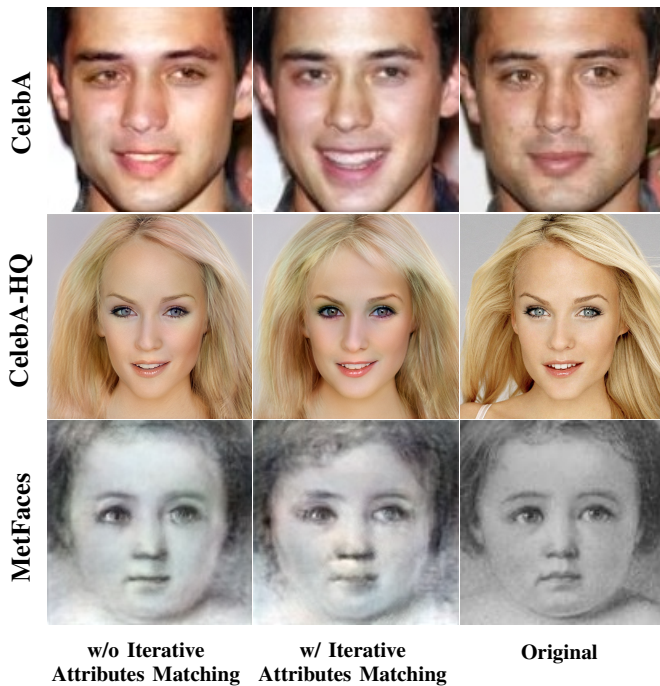


Fig. 10: Qualitative results on whether the iterative attributes matching mechanism is incorporated into Editable-DeepSC. The instructive sentences for the 1st, 2nd, and 3rd rows are “Smile more”, “What about trying bangs that leaves half of the forehead visible”, and “Make the bangs longer”.

TABLE VI: The numbers of parameters in various parts of Editable-DeepSC. We also report the ratio of tuned parameters.

Frozen Parameters	Tuned Parameters	Total Parameters	Tuned Ratio
$7.70 \times 10^7$	$0.21 \times 10^7$	$7.91 \times 10^7$	<b>2.65%</b>

than 1600 MiB GPU memory for the resolution of  $128 \times 128$  and less than 3000 MiB GPU memory for the resolution of  $1024 \times 1024$ . Thus, Editable-DeepSC achieves a good trade-off between utility and efficiency.

**Parameters analysis.** From Table VI, we note that the fine-tuned parameters only take up 2.65% of the total, while the remaining 97.35% of the total parameters are kept frozen. Nonetheless, the fine-tuning mechanism still results in significant performance gains. This further confirms the practicality and effectiveness of our fine-tuning method.

## VI. CONCLUSION

In this paper, we propose Editable-DeepSC, a novel cross-modal semantic communication approach that tackles the communication challenges under dynamic facial editing scenarios in a conversational and interactive way. Specifically, we first theoretically analyze different transmission schemes that separately handle communications and editings. We find that they actually increase the data processing procedures and are more likely to lose semantic mutual information. In light of this, we emphasize the necessity to integrate editings into the communication chain, jointly optimize these two aspects, and preserve more semantic mutual information. To compress

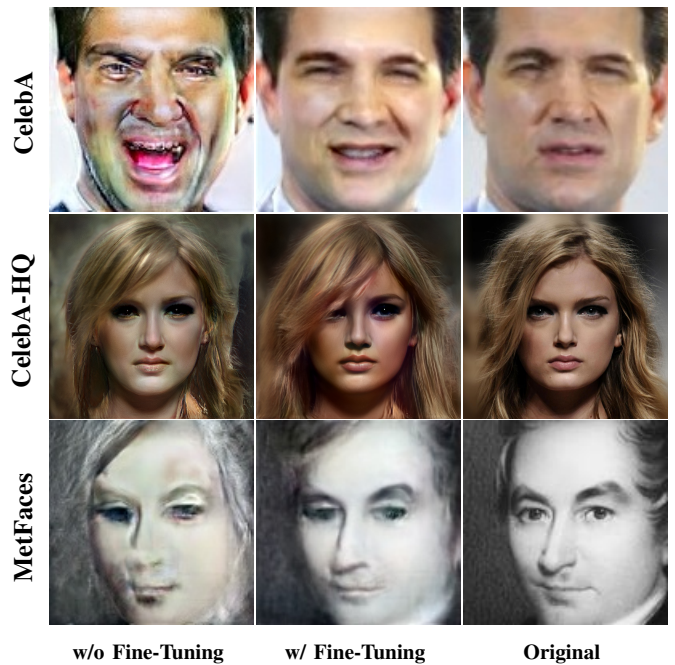


Fig. 11: Qualitative results on whether the fine-tuning mechanism is incorporated into Editable-DeepSC. The instructive sentences for the 1st, 2nd, and 3rd rows are “Smile more”, “Add long bangs”, and “Make the fringe just a little longer”.

the high-dimensional data, we leverage inversion methods based on pre-trained StyleGAN priors for semantic coding. To tackle the dynamic channel noise conditions, we propose SNR-aware channel coding based on model fine-tuning, which introduces two lightweight trainable adapters to capture the distribution of new noise conditions. Extensive experiments demonstrate that compared to existing methods, Editable-DeepSC exhibits superior editing effects while significantly saving the transmission bandwidth under multiple settings.

APPENDIX A  
PROOF OF THEOREM 1

We denote the sampled variables of  $U$ ,  $V$ ,  $W$  as  $u$ ,  $v$ ,  $w$ , respectively. Firstly, we expand the mutual information term:

$$\begin{aligned}
\mathcal{I}(U; V, W) &= \int_U \int_V \int_W p(u, v, w) \\
&\cdot \log \left( \frac{p(u, v, w)}{p(u) \cdot p(v, w)} \right) dudvdw \\
&= \int_U p(u) \left( \int_V \int_W \frac{p(u, v, w)}{p(u)} \right. \\
&\cdot \log \left( \frac{p(u, v, w)/p(u)}{p(v, w)} \right) dvdw \Big) du \\
&= \int_U p(u) \left( \int_V \int_W p(v, w|u) \right. \\
&\cdot \log \left( \frac{p(v, w|u)}{p(v, w)} \right) dvdw \Big) du \\
&= \int_U p(u) \left( \int_V \int_W p(v|u) \cdot p(w|v, u) \right. \\
&\cdot \log \left( \frac{p(v|u) \cdot p(w|v, u)}{p(v) \cdot p(w|v)} \right) dvdw \Big) du \\
&= \int_U p(u) \left( \int_V \int_W p(v|u) \cdot p(w|v, u) \right. \\
&\cdot \log \left( \frac{p(v|u)}{p(v)} \right) dvdw \Big) du \\
&+ \int_U p(u) \left( \int_V \int_W p(v|u) \cdot p(w|v, u) \right. \\
&\cdot \log \left( \frac{p(w|v, u)}{p(w|v)} \right) dvdw \Big) du \\
&= \int_U p(u) \left( \int_V p(v|u) \right. \\
&\cdot \log \left( \frac{p(v|u)}{p(v)} \right) \cdot \left( \int_W p(w|v, u) dw \right) dv \Big) du \\
&+ \int_U \int_V \int_W p(u, v, w) \\
&\cdot \log \left( \frac{p(w|v, u)}{p(w|v)} \right) dudvdw.
\end{aligned}
\tag{19}$$

Given that  $\int_W p(w|v, u)dw = 1$ , the first term of the last expression in (19) can be further simplified as

$$\begin{aligned}
&\int_U p(u) \left( \int_V p(v|u) \right. \\
&\cdot \log \left( \frac{p(v|u)}{p(v)} \right) \cdot \left( \int_W p(w|v, u) dw \right) dv \Big) du \\
&= \int_U p(u) \left( \int_V p(v|u) \cdot \log \left( \frac{p(v|u)}{p(v)} \right) dv \right) du \\
&= \int_U \int_V p(u) \cdot p(v|u) \cdot \log \left( \frac{p(u) \cdot p(v|u)}{p(u) \cdot p(v)} \right) dudv \\
&= \int_U \int_V p(u, v) \cdot \log \left( \frac{p(u, v)}{p(u) \cdot p(v)} \right) dudv \\
&= \mathcal{I}(U; V),
\end{aligned}
\tag{20}$$

while the second term of (19) can also be transformed into

$$\begin{aligned}
&\int_U \int_V \int_W p(u, v, w) \\
&\cdot \log \left( \frac{p(w|v, u)}{p(w|v)} \right) dudvdw \\
&= \int_V p(v) \left( \int_U \int_W p(u, w|v) \right. \\
&\cdot \log \left( \frac{p(w|v, u)}{p(w|v)} \right) dudw \Big) dv \\
&= \int_V p(v) \left( \int_U \int_W p(u, w|v) \right. \\
&\cdot \log \left( \frac{p(u|v) \cdot p(w|v, u)}{p(u|v) \cdot p(w|v)} \right) dudw \Big) dv \\
&= \int_V p(v) \left( \int_U \int_W p(u, w|v) \right. \\
&\cdot \log \left( \frac{p(u, w|v)}{p(u|v) \cdot p(w|v)} \right) dudw \Big) dv \\
&= \mathcal{I}(U; W|V).
\end{aligned}
\tag{21}$$

By combining the results of (20) and (21) into (19), we have

$$\mathcal{I}(U; V, W) = \mathcal{I}(U; V) + \mathcal{I}(U; W|V), \tag{22}$$

and by conducting similar derivations, we also have

$$\mathcal{I}(U; V, W) = \mathcal{I}(U; W) + \mathcal{I}(U; V|W). \tag{23}$$

Note that  $U$ ,  $V$ ,  $W$  satisfy the Markov process  $U \rightarrow V \rightarrow W$ . Thus, when  $V$  is given,  $U$  and  $W$  are conditionally independent, which implies that  $\mathcal{I}(U; W|V) = 0$ . Moreover, the mutual information term inherently has the characteristic of non-negativity, which means that  $\mathcal{I}(U; V|W) \geq 0$ . Consequently, we convert the results of (22) and (23) into:

$$\begin{aligned}
\mathcal{I}(U; V) &= \mathcal{I}(U; V) + 0 = \mathcal{I}(U; V) + \mathcal{I}(U; W|V) \\
&= \mathcal{I}(U; V, W) \\
&= \mathcal{I}(U; W) + \mathcal{I}(U; V|W) \\
&\geq \mathcal{I}(U; W) + 0 = \mathcal{I}(U; W).
\end{aligned}
\tag{24}$$

This concludes the proof.

REFERENCES

- [1] W. Yu, B. Chen, Q. Zhang, and S.-T. Xia, "Editable-deepscc: Cross-modal editable semantic communication systems," in *2024 IEEE 99th Vehicular Technology Conference (VTC2024-Spring)*. IEEE, 2024, pp. 1–5.
- [2] G. Chryssolouris, D. Mavrikios, N. Papakostas, D. Mourtzis, G. Michalos, and K. Georgoulas, "Digital manufacturing: history, perspectives, and outlook," *Proceedings of the Institution of Mechanical Engineers, Part B: Journal of Engineering Manufacture*, vol. 223, no. 5, pp. 451–462, 2009.
- [3] C. O. Alenoghena, H. O. Ohize, A. O. Adejo, A. J. Onumanyi, E. E. Ohiohin, A. I. Balarabe, S. A. Okoh, E. Kolo, and B. Alenoghena, "Telemedicine: A survey of telecommunication technologies, developments, and challenges," *Journal of Sensor and Actuator Networks*, vol. 12, no. 2, p. 20, 2023.
- [4] M. Soori, B. Arezoo, and R. Dastres, "Artificial intelligence, machine learning and deep learning in advanced robotics, a review," *Cognitive Robotics*, vol. 3, pp. 54–70, 2023.

- [5] H. Wang, H. Ning, Y. Lin, W. Wang, S. Dhelim, F. Farha, J. Ding, and M. Daneshmand, "A survey on the metaverse: The state-of-the-art, technologies, applications, and challenges," *IEEE Internet of Things Journal*, vol. 10, no. 16, pp. 14 671–14 688, 2023.
- [6] H. Zhang, S. Shao, M. Tao, X. Bi, and K. B. Letaief, "Deep learning-enabled semantic communication systems with task-unaware transmitter and dynamic data," *IEEE Journal on Selected Areas in Communications*, vol. 41, no. 1, pp. 170–185, 2023.
- [7] D. Huang, F. Gao, X. Tao, Q. Du, and J. Lu, "Toward semantic communications: Deep learning-based image semantic coding," *IEEE Journal on Selected Areas in Communications*, vol. 41, no. 1, pp. 55–71, 2022.
- [8] C. Dong, H. Liang, X. Xu, S. Han, B. Wang, and P. Zhang, "Semantic communication system based on semantic slice models propagation," *IEEE Journal on Selected Areas in Communications*, vol. 41, no. 1, pp. 202–213, 2022.
- [9] T.-Y. Tung and D. Gündüz, "Deepwive: Deep-learning-aided wireless video transmission," *IEEE Journal on Selected Areas in Communications*, vol. 40, no. 9, pp. 2570–2583, 2022.
- [10] P. Jiang, C.-K. Wen, S. Jin, and G. Y. Li, "Wireless semantic communications for video conferencing," *IEEE Journal on Selected Areas in Communications*, vol. 41, no. 1, pp. 230–244, 2022.
- [11] S. Wang, J. Dai, Z. Liang, K. Niu, Z. Si, C. Dong, X. Qin, and P. Zhang, "Wireless deep video semantic transmission," *IEEE Journal on Selected Areas in Communications*, vol. 41, no. 1, pp. 214–229, 2022.
- [12] H. Xie, Z. Qin, and G. Y. Li, "Task-oriented multi-user semantic communications for vqa," *IEEE Wireless Communications Letters*, vol. 11, no. 3, pp. 553–557, 2021.
- [13] H. Xie, Z. Qin, X. Tao, and K. B. Letaief, "Task-oriented multi-user semantic communications," *IEEE Journal on Selected Areas in Communications*, vol. 40, no. 9, pp. 2584–2597, 2022.
- [14] P. Wang, J. Li, M. Ma, and X. Fan, "Distributed audio-visual parsing based on multimodal transformer and deep joint source channel coding," in *ICASSP 2022-2022 IEEE International Conference on Acoustics, Speech and Signal Processing (ICASSP)*. IEEE, 2022, pp. 4623–4627.
- [15] H. Yang, D. Huang, Y. Wang, and A. K. Jain, "Learning face age progression: A pyramid architecture of gans," in *Proceedings of the IEEE conference on computer vision and pattern recognition*, 2018, pp. 31–39.
- [16] K. Olszewski, D. Ceylan, J. Xing, J. Echevarria, Z. Chen, W. Chen, and H. Li, "Intuitive, interactive beard and hair synthesis with generative models," in *Proceedings of the IEEE/CVF Conference on Computer Vision and Pattern Recognition*, 2020, pp. 7446–7456.
- [17] W. Wang, X. Alameda-Pineda, D. Xu, P. Fua, E. Ricci, and N. Sebe, "Every smile is unique: Landmark-guided diverse smile generation," in *Proceedings of the IEEE Conference on Computer Vision and Pattern Recognition*, 2018, pp. 7083–7092.
- [18] Y. Shen, J. Gu, X. Tang, and B. Zhou, "Interpreting the latent space of gans for semantic face editing," in *Proceedings of the IEEE/CVF conference on computer vision and pattern recognition*, 2020, pp. 9243–9252.
- [19] P. Zhuang, O. Koyejo, and A. G. Schwing, "Enjoy your editing: Controllable gans for image editing via latent space navigation," in *9th International Conference on Learning Representations, ICLR 2021*, 2021.
- [20] Y. Jiang, Z. Huang, T. Wu, X. Pan, C. C. Loy, and Z. Liu, "Talk-to-edit: Fine-grained 2d and 3d facial editing via dialog," *IEEE Transactions on Pattern Analysis and Machine Intelligence*, vol. 46, no. 5, pp. 3692–3706, 2024.
- [21] I. Goodfellow, J. Pouget-Abadie, M. Mirza, B. Xu, D. Warde-Farley, S. Ozair, A. Courville, and Y. Bengio, "Generative adversarial networks," *Communications of the ACM*, vol. 63, no. 11, pp. 139–144, 2020.
- [22] W. Xia, Y. Zhang, Y. Yang, J.-H. Xue, B. Zhou, and M.-H. Yang, "Gan inversion: A survey," *IEEE transactions on pattern analysis and machine intelligence*, vol. 45, no. 3, pp. 3121–3138, 2022.
- [23] Y. Qiu, H. Yu, H. Fang, W. Yu, B. Chen, X. Wang, S.-T. Xia, and K. Xu, "Mibench: A comprehensive benchmark for model inversion attack and defense," *arXiv preprint arXiv:2410.05159*, 2024.
- [24] Y. Qiu, H. Fang, H. Yu, B. Chen, M. Qiu, and S.-T. Xia, "A closer look at gan priors: Exploiting intermediate features for enhanced model inversion attacks," *arXiv preprint arXiv:2407.13863*, 2024.
- [25] H. Fang, Y. Qiu, H. Yu, W. Yu, J. Kong, B. Chong, B. Chen, X. Wang, S.-T. Xia, and K. Xu, "Privacy leakage on dnns: A survey of model inversion attacks and defenses," *arXiv preprint arXiv:2402.04013*, 2024.
- [26] T. Karras, S. Laine, and T. Aila, "A style-based generator architecture for generative adversarial networks," in *Proceedings of the IEEE/CVF conference on computer vision and pattern recognition*, 2019, pp. 4401–4410.
- [27] E. Boursoulatzé, D. B. Kurka, and D. Gündüz, "Deep joint source-channel coding for wireless image transmission," *IEEE Transactions on Cognitive Communications and Networking*, vol. 5, no. 3, pp. 567–579, 2019.
- [28] Z. Chen, Y. Duan, W. Wang, J. He, T. Lu, J. Dai, and Y. Qiao, "Vision transformer adapter for dense predictions," in *The Eleventh International Conference on Learning Representations*, 2023.
- [29] H. Chen, R. Tao, H. Zhang, Y. Wang, X. Li, W. Ye, J. Wang, G. Hu, and M. Savvides, "Conv-adapter: Exploring parameter efficient transfer learning for convnets," in *Proceedings of the IEEE/CVF Conference on Computer Vision and Pattern Recognition*, 2024, pp. 1551–1561.
- [30] M. Wang, X.-Q. Lyu, Y.-J. Li, and F.-L. Zhang, "Vr content creation and exploration with deep learning: A survey," *Computational Visual Media*, vol. 6, pp. 3–28, 2020.
- [31] F. Arena, M. Collotta, G. Pau, and F. Termini, "An overview of augmented reality," *Computers*, vol. 11, no. 2, p. 28, 2022.
- [32] S. Ryu, K. Ko, and J. W.-K. Hong, "Performance analysis of applying deep learning for virtual background of webrtc-based video conferencing system," in *2021 22nd Asia-Pacific Network Operations and Management Symposium (APNOMS)*. IEEE, 2021, pp. 53–56.
- [33] W. Yu, H. Fang, B. Chen, X. Sui, C. Chen, H. Wu, S.-T. Xia, and K. Xu, "Gi-nas: Boosting gradient inversion attacks through adaptive neural architecture search," *arXiv preprint arXiv:2405.20725*, 2024.
- [34] H. Fang, B. Chen, X. Wang, Z. Wang, and S.-T. Xia, "Gifd: A generative gradient inversion method with feature domain optimization," in *Proceedings of the IEEE/CVF International Conference on Computer Vision*, 2023, pp. 4967–4976.
- [35] H. Fang, J. Kong, B. Chen, T. Dai, H. Wu, and S.-T. Xia, "Clip-guided generative networks for transferable targeted adversarial attacks," in *European Conference on Computer Vision*. Springer, 2025, pp. 1–19.
- [36] H. Yu, Y. Qiu, H. Fang, B. Chen, S. Yu, B. Wang, S.-T. Xia, and K. Xu, "Calor: Towards comprehensive model inversion defense," *arXiv preprint arXiv:2410.05814*, 2024.
- [37] Y. Tan, Y. Peng, H. Fang, B. Chen, and S.-T. Xia, "Waterdiff: Perceptual image watermarks via diffusion model," in *ICASSP 2024-2024 IEEE International Conference on Acoustics, Speech and Signal Processing (ICASSP)*. IEEE, 2024, pp. 3250–3254.
- [38] X. Zhong, H. Fang, B. Chen, X. Gu, T. Dai, M. Qiu, and S.-T. Xia, "Hierarchical features matter: A deep exploration of gan priors for improved dataset distillation," *arXiv preprint arXiv:2406.05704*, 2024.
- [39] L. P. Kaelbling, M. L. Littman, and A. W. Moore, "Reinforcement learning: A survey," *Journal of artificial intelligence research*, vol. 4, pp. 237–285, 1996.
- [40] D. A. Hudson and C. D. Manning, "Compositional attention networks for machine reasoning," in *International Conference on Learning Representations*, 2018.
- [41] A. Vaswani, "Attention is all you need," *Advances in Neural Information Processing Systems*, 2017.
- [42] E. Erdemir, T.-Y. Tung, P. L. Dragotti, and D. Gündüz, "Generative joint source-channel coding for semantic image transmission," *IEEE Journal on Selected Areas in Communications*, vol. 41, no. 8, pp. 2645–2657, 2023.
- [43] S. F. Yılmaz, C. Karamanlı, and D. Gündüz, "Distributed deep joint source-channel coding over a multiple access channel," in *ICC 2023-IEEE International Conference on Communications*. IEEE, 2023, pp. 1400–1405.
- [44] T.-Y. Tung and D. Gündüz, "Deep joint source-channel and encryption coding: Secure semantic communications," in *ICC 2023-IEEE International Conference on Communications*. IEEE, 2023, pp. 5620–5625.
- [45] N. Tishby and N. Zaslavsky, "Deep learning and the information bottleneck principle," in *2015 IEEE information theory workshop (itw)*. IEEE, 2015, pp. 1–5.
- [46] A. M. Saxe, Y. Bansal, J. Dapello, M. Advani, A. Kolchinsky, B. D. Tracey, and D. D. Cox, "On the information bottleneck theory of deep learning," in *International Conference on Learning Representations*, 2018.
- [47] T. M. Cover, *Elements of information theory*. John Wiley & Sons, 1999.
- [48] R. Zhang, P. Isola, A. A. Efros, E. Shechtman, and O. Wang, "The unreasonable effectiveness of deep features as a perceptual metric," in *Proceedings of the IEEE conference on computer vision and pattern recognition*, 2018, pp. 586–595.
- [49] Y. Jiang, Z. Huang, X. Pan, C. C. Loy, and Z. Liu, "Talk-to-edit: Fine-grained facial editing via dialog," in *Proceedings of the IEEE/CVF International Conference on Computer Vision*, 2021, pp. 13 799–13 808.

- [50] S. Hochreiter, “Long short-term memory;” *Neural Computation MIT-Press*, 1997.
- [51] J. Deng, J. Guo, N. Xue, and S. Zafeiriou, “Arcface: Additive angular margin loss for deep face recognition,” in *Proceedings of the IEEE/CVF conference on computer vision and pattern recognition*, 2019, pp. 4690–4699.
- [52] Z. Liu, P. Luo, X. Wang, and X. Tang, “Deep learning face attributes in the wild,” in *Proceedings of the IEEE international conference on computer vision*, 2015, pp. 3730–3738.
- [53] T. Karras, T. Aila, S. Laine, and J. Lehtinen, “Progressive growing of gans for improved quality, stability, and variation;” in *International Conference on Learning Representations*, 2018.
- [54] T. Karras, M. Aittala, J. Hellsten, S. Laine, J. Lehtinen, and T. Aila, “Training generative adversarial networks with limited data,” *Advances in neural information processing systems*, vol. 33, pp. 12 104–12 114, 2020.
- [55] G. K. Wallace, “The jpeg still picture compression standard,” *IEEE transactions on consumer electronics*, vol. 38, no. 1, pp. xviii–xxxiv, 1992.
- [56] R. Gallager, “Low-density parity-check codes,” *IRE Transactions on information theory*, vol. 8, no. 1, pp. 21–28, 1962.
- [57] M. Heusel, H. Ramsauer, T. Unterthiner, B. Nessler, and S. Hochreiter, “Gans trained by a two time-scale update rule converge to a local nash equilibrium,” *Advances in neural information processing systems*, vol. 30, 2017.
- [58] M. Bińkowski, D. J. Sutherland, M. Arbel, and A. Gretton, “Demystifying mmd gans;” in *International Conference on Learning Representations*, 2018.